N-Methylated Macrobicyclic Hexaamines of Copper(II) and Nickel(II): Large Steric Effects

Paul V. Bernhardt,[1,*] Jack M. Harrowfield,[2,*] David C. R. Hockless,[1,*] and Alan M. Sargeson[1,*]

Research School of Chemistry, Australian National University, Canberra, ACT, 0200, Australia, and Department of Physical and Inorganic Chemistry, University of Western Australia, Nedlands, WA, 6009, Australia

Received June 8, 1994[⊗]

Complexation of the penta-, hexa- and hepta-N-methylated derivatives of the macrobicyclic hexaamine sar (3,6,-10,13,16,19-hexaaza-bicyclo[6.6.6]icosane) with nickel(II) and copper(II) is reported. Unlike their analogous hexadentate-coordinated $[M(sar)]^{2+}$ complexes, the Cu(II) and Ni(II) complexes of N-Me$_5$sar, N-Me$_6$sar and N-Me$_7$-sar$^+$ show the ligands coordinating only as tetradentates, both in the solid state and in solution. The X-ray crystallographic analyses of $[Ni(N\text{-}Me_5sar)](ClO_4)_2$, orthorhombic, space group $P2_12_12_1$, a 9.915(2), b 10.694(2), c 25.549(6) Å, $Z = 4$; $\{[Ni(HN\text{-}Me_6sar)](ClO_4)_3 \cdot 2H_2O\}_3$, triclinic, space group $P\bar{1}$, a 14.160(2), b 17.739(4), c 21.617(5) Å, α 75.20(2), β 89.72(2), γ 68.31(1)°, $Z = 2$; $[Ni(N\text{-}Me_7sar)](ClO_4)_3$, orthorhombic, space group $P2_12_12_1$, a 10.752(2), b 13.410(2), c 21.643(3) Å, $Z = 4$; $[Cu(N\text{-}Me_5sar)](ClO_4)_2$, orthorhombic, space group $P2_12_12_1$, a 10.005(1), b 10.524(1), c 25.731(2) Å, $Z = 4$ and $[Cu(N\text{-}Me_7sar)](ClO_4)_3 \cdot 0.5H_2O$, orthorhombic, space group $P2_12_12_1$, a 11.337(2), b 12.802(2), c 22.170(2) Å, $Z = 4$, are reported. The Ni(II) complexes exhibit marked solvent, temperature and pH-dependent electronic spectra as a result of high-spin/low-spin equilibria. Molecular mechanics calculations indicate that hexadentate coordination of N-Me$_6$sar to metal ions such as Cu-(II) and Ni(II) will be unfavorable as a result of severe steric strain.

Introduction

A feature of the macrobicyclic hexaamine sar is its propensity to coordinate to a wide variety of metal ions as a hexadentate.[3] The resulting hexaamine complexes are, in general, quite resistant to dissociation, so tetradentate coordination of ligands based on sar has been a rare occurrence. One example in which tetradentate coordination has been positively identified is an intermediate in the acid-catalyzed dissociation of $[Cu(sar)]^{n+}$, where the ligand is bound initially as a hexadentate, but undergoes rapid protonation to yield a tetradentate coordinated complex, $[Cu(H_2sar)](NO_3)_4$, which has been characterized by an X-ray crystallographic analysis.[4] Other configurational isomers of the tetradentate coordinated complex have been proposed to occur in the demetalation process, but their precise identification has been difficult to establish due to facile interconversions.

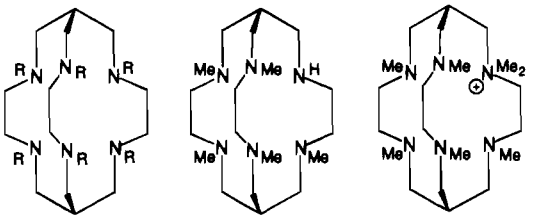

Often N-alkylation of secondary polyamines effects a quite dramatic change on their coordination chemistry. For example, N-methylation invariably results in a positive shift in the M(II/I) redox couple and an extension of the metal-nitrogen (M–N) bond relative to the secondary amine parent. In addition, the reactivities of complexes of tertiary polyamines are quite characteristic, where complex formation,[5] conformational interconversions[6] and N-based isomerization reactions[7] generally occur much less readily than in secondary amine analogues. However, the severe steric strain that is introduced upon N-methylation of a coordinated secondary amine has resulted in there being no known example of a hexaamine complex where all N-donors are tertiary amines. Since sar shows such a strong preference toward hexadentate coordination, the N-methylated analogue N-Me$_6$sar also appeared to be a likely candidate for hexadentate coordination. A preliminary investigation of the copper(II) chemistry of N-Me$_6$sar resulted in the isolation and structural characterization of a complex where the ligand had formally eliminated ethylene from one 'strap' and was bound as a tetradentate.[8] The coordination of N-Me$_6$sar to nickel(II) and copper(II) has now been investigated in full, along with parallel studies on the analogs N-Me$_5$sar and the alkyl ammonium cation N-Me$_7$sar$^+$.

Experimental Section

Safety Note. Although we have experienced no problems with the compounds reported in this work, perchlorate salts are potentially explosive, and should only be handled in small quantities, never heated in the solid state nor scraped away from sintered glass frits.

Syntheses. 3,6,10,13,16,19-Hexamethyl-3,6,10,13,16,19-hexaaza-bicyclo[6.6.6]icosane (N-Me$_6$sar) was prepared as described,[9] except the crude product, which was found to contain both N-Me$_5$sar and [N-Me$_7$sar]I, was not recrystallized. When desired, purification was

⊗ Abstract published in *Advance ACS Abstracts,* November 1, 1994.

(1) Australian National University.
(2) University of Western Australia.
(3) Comba, P.; Sargeson, A. M.; Engelhardt, L. M.; Harrowfield, J. M.; White, A. H.; Horn, E.; Snow, M. R. *Inorg. Chem.* **1985**, *24*, 2325.
(4) Sargeson, A. M. *Pure Appl. Chem.* **1986**, *58*, 1511. White, A. H. unpublished results.
(5) Röper, J. R.; Elias, H. *Inorg. Chem.* **1992**, *31*, 1202.
(6) Hawkins, C. J.; Peachey, R. M. *Aust. J. Chem.* **1976**, *29*, 33.
(7) Freeman, G. M.; Barefield, E. K.; van Derveeer, D. G. *Inorg. Chem.* **1984**, *23*, 3092.
(8) Harrowfield, J. M.; Sargeson, A. M.; Skelton, B. W.; White, A. H. *Aust. J. Chem.* **1994**, *47*, 181.

0020-1669/94/1333-5659$04.50/0 © 1994 American Chemical Society

Table 1. Crystal Data

	$[Ni(N\text{-}Me_5sar)](ClO_4)_2$	$\{[Ni(HN\text{-}Me_6sar)](ClO_4)_3\}_3$	$[Ni(N\text{-}Me_7sar)](ClO_4)_3$	$[Cu(N\text{-}Me_5sar)](ClO_4)_2$	$[Cu(N\text{-}Me_7sar)](ClO_4)_3{\cdot}0.5H_2O$
Formula	$C_{19}H_{42}Cl_2N_6NiO_8$	$C_{60}H_{147}C_{19}N_{18}Ni_3O_{42}$	$C_{21}H_{47}Cl_3N_6NiO_{12}$	$C_{19}H_{42}Cl_2CuN_6O_8$	$C_{21}H_{47}Cl_3CuN_6O_{12.5}$
a, Å	9.915(2)	14.160(2)	10.752(2)	10.005(1)	11.337(2)
b, Å	10.694(2)	17.739(4)	13.410(2)	10.425(1)	12.802(2)
c, Å	25.549(6)	21.617(5)	21.643(3)	25.731(2)	22.170(2)
α, deg		75.20(2)			
β, deg		89.72(2)			
γ, deg		68.31(1)			
V, Å^3	2709.0(9)	4853(1)	3120.7(8)	2709.3(4)	3217.6(7)
Z	4	2	4	4	4
fw	612.18	2288.09	740.69	617.43	753.54
space group	$P2_12_12_1$ (No. 19)	$P\bar{1}$ (No. 2)	$P2_12_12_1$ (No. 19)	$P2_12_12_1$ (No. 19)	$P2_12_12_1$ (No. 19)
temp, °C	23	−60	23	23	−60
λ, Å	1.54178	1.54178	1.54178	1.54178	1.54178
ϱ_{calcd}, g cm^{-3}	1.501	1.565	1.576	1.513	1.555
μ, cm^{-1}	33.15	37.85	38.58	34.20	38.49
$R(F_o)$, $R_w(F_o)$[a]	0.037, 0.026	0.090, 0.104	0.045, 0.046	0.031, 0.026	0.079, 0.074

[a] $R(F_o) = \sum(||F_o| - |F_c||)/\sum|F_o|$, $R_w(F_o) = (\sum w(|F_o| - |F_c|)^2/\sum wF_o^2)^{1/2}$.

achieved by suspending the crude product (*ca.* 2.0 g) in water (10 mL) then stirring at 80° for 15 min. Following cooling to *ca.* 40°, pure N-Me$_6$sar was collected by filtration as a colorless powder and dried in a vacuum desiccator (1.0 g). Anal. Calcd for $C_{20}H_{45}N_6O_{0.5}$: C, 63.61; H, 12.01; N, 22.26. Found: C, 63.47; H, 12.67; N, 22.51. All other reagents were of analytical purity.

Nickel(II) Complexes. To a solution of nickel(II) chloride hexahydrate (1.47 g, 6.2 mmol) in water (50 mL) was added crude N-Me$_6$sar (2.70 g, ~6.2 mmol) and the suspension was refluxed for 3 d. The reaction mixture was diluted to 500 mL, filtered and sorbed on a column (20 × 3 cm) of SP-Sephadex C25 cation exchange resin (Na^+ form). The eluent was 0.25 M Na_2HPO_4. Three bands were removed; the order being green, yellow, then green. The eluate from each band was diluted five-fold with water and rechromatographed, individually, on a Sephadex column as above except 0.5 M $NaClO_4$ was employed as the eluent.

Band 1. $[Ni(N\text{-}Me_6sar)](ClO_4)_2{\cdot}2H_2O$. This fraction was concentrated to *ca.* 100 mL, which resulted in a color change of the solution from green to red, and dark red crystals formed on standing. These were collected by filtration (see Safety Note), washed with ethanol then diethyl ether and dried in a vacuum desiccator (0.8 g, 20%). Anal. Calcd for $C_{20}H_{44}Cl_2N_6NiO_8$: C, 38.36; H, 7.08; N, 13.42; Cl, 11.32. Found: C, 38.08; H, 7.50; N, 13.20; Cl, 11.28. Crystallization from slightly acidic solution (pH ~ 4) produced red prisms of the protonated complex $[Ni(HN\text{-}Me_6sar)](ClO_4)_3{\cdot}2H_2O$ which were suitable for X-ray analysis.

Band 2. $[Ni(N\text{-}Me_5sar)](ClO_4)_2$. The eluate was concentrated to *ca.* 150 mL and the pH of the solution was adjusted to *ca.* 8 with NaOH solution. Orange rod-shaped crystals formed on standing, which were suitable for X-ray studies. These were collected by filtration (see Safety Note), washed with ethanol then diethyl ether and dried in a vacuum desiccator (0.5 g, 11%). Anal. Calcd for $C_{19}H_{42}Cl_2N_6NiO_8$: C, 37.28; H, 6.92; N, 13.73; Cl, 11.58 . Found: C, 37.89; H, 7.37; N, 13.73; Cl, 11.68. The protonated complex $[Ni(HN\text{-}Me_5sar)](ClO_4)_3$, isolated from mildly acidic perchlorate solution (pH ~ 4), crystallizes as yellow/orange octahedral prisms. Anal. Calcd for $C_{19}H_{43}Cl_3N_6NiO_{12}$: C, 32.02; H, 6.08; N, 11.79; Cl, 14.92. Found: C, 31.78; H, 6.17; N, 11.60; Cl, 14.90. NMR (D_2O): ^1H δ 2.24 (s, CH_3), ~2.40 (s (br), CH_2), 2.44 (s, CH_3), 2.60 (s, CH_3), ~2.50 (mult., CH_2), ~2.86 (mult., CH_2), ~3.24 (mult., CH_2), 3.16 (s, CH_3), 3.22 (s, CH_3), ~3.30 (mult., CH_2), 3.70 (s (br), CH). ^{13}C δ 35.4, 39.1, 43.9, 44.8, 48.3, 48.8, 49.3, 57.4, 59.0, 59.1, 59.7, 61.0, 62.3, 63.9.

Band 3. $[Ni(N\text{-}Me_7sar)](ClO_4)_3{\cdot}H_2O$. This band was concentrated to *ca.* 30 mL, which resulted in a color change from green to yellow and eventually precipitation of the product as orange prisms suitable for X-ray analysis. These were collected by filtration (see Safety Note), washed with ethanol then diethyl ether and dried in a vacuum desiccator (0.06 g, 1%). Anal. Calcd for $C_{21}H_{49}Cl_3N_6NiO_{13}$: C, 33.24; H, 6.51; N, 11.08; Cl, 14.02. Found: C, 33.50; H, 6.52; N, 11.15; Cl, 14.51.

Copper(II) Complexes. A solution of crude N-Me$_6$sar (1.61 g, ~3.7 mmol) and copper(II) nitrate trihydrate (0.90 g, 3.6 mmol) in methanol (75 mL) was refluxed for 16 h. After cooling, the solution was diluted to 1 L with water, filtered and sorbed on a Sephadex column (see above). Two bands were separated with 0.5 M $NaClO_4$ solution.

Band 1. $[Cu(N\text{-}Me_5sar)](ClO_4)_2$/$[Cu(N\text{-}Me_6sar)](ClO_4)_2$. This band was diffuse, with the front being blue (λ_{max} 588 nm) and the tail being purple (λ_{max} 552 nm). Concentration to *ca.* 20 mL afforded precipitation of the mixture of complexes as a purple powder. This was collected by filtration (see Safety Note), washed with ethanol then diethyl ether and dried in a vacuum desiccator (0.8 g, 35 %). A solution of this mixture (0.7 g) in water (50 mL) was sorbed on a 90 × 3 cm Sephadex C-25 column (Na^+ form). This is the maximum recommended loading to achieve separation of the two complexes. The eluent was 0.3 M $NaClO_4$, which resulted in two close running bands; the first blue ($[Cu(N\text{-}Me_6sar)]^{2+}$) and the second purple ($[Cu(N\text{-}Me_5sar)]^{2+}$). A minor purple band eluted well behind the first two, which resulted from an equilibrium between the aqua and perchlorato complexes of the two species (see Results section). These were both concentrated to *ca.* 20 mL and crystallization occurred on standing. The solids were collected by filtration (see Safety Note), washed with ethanol then diethyl ether and dried in a vacuum desiccator. Typically, *ca.* 0.25 g of each complex was recovered from the overall workup. Magenta crystals of $[Cu(N\text{-}Me_5sar)](ClO_4)_2$, suitable for X-ray analysis, formed by slow evaporation of the filtrate remaining after the initial precipitate had been collected. Anal. $[Cu(N\text{-}Me_6sar)](ClO_4)_2$: Calcd for $C_{20}H_{46}Cl_2CuN_6O_9$: C, 37.01; H, 7.14; N, 12.95; Cl, 10.92. Found: C, 37.41; H, 7.18; N, 12.77; Cl, 11.22. $[Cu(N\text{-}Me_5sar)](ClO_4)_2{\cdot}0.5H_2O$: Calcd for $C_{19}H_{43}Cl_2CuN_6O_{8.5}$: C, 36.46; H, 6.92; N, 14.43; Cl, 11.33. Found: C, 36.76 H, 6.77; N, 13.09; Cl, 11.31.

Band 2. $[Cu(N\text{-}Me_7sar)](ClO_4)_3{\cdot}H_2O$. This band (blue) was well separated from the first diffuse band and, following concentration to 50 mL, afforded lustrous dark blue crystals on standing which were suitable for X-ray analysis. These were collected by filtration (see Safety Note), washed with ethanol then diethyl ether and dried in a vacuum desiccator (0.2 g, 7%). Anal. Calcd for $C_{21}H_{49}Cl_3CuN_6O_{13}$: C, 33.03; H, 6.47; N, 11.01; Cl, 13.93. Found: C, 32.92; H, 6.52; N, 10.96; Cl, 14.34.

Several crops were obtained from each of the above fractions, but coprecipitation of sodium perchlorate contaminated later crops, thus diminishing the overall yield of pure complex somewhat.

Physical Methods. Electronic spectra were recorded with a Hewlett-Packard 8450A UV-vis spectrophotometer. NMR spectra were recorded with a Varian GEMINI 300 spectrometer at 300 (^1H) and 75 (^{13}C) MHz, with all chemical shifts being cited versus tetramethylsilane. EPR spectra were measured at 40K with a Varian V-4502 spectrometer employing a V-4561 34.99 GHz microwave bridge, with all samples being *ca.* 1 mM frozen solutions in DMF:H_2O 1:2. Spin Hamiltonian parameters were determined by fitting each spectrum with the simulation program EPR50F.[10] Electrochemical measurements were made with

(9) Bottomley, G. A.; Clark, I. J.; Creaser, I. I.; Engelhardt, L. M.; Geue, R. J.; Hagen, K. S.; Harrowfield, J. M.; Lawrance, G. A.; Lay, P. A.; Sargeson, A. M.; See, A. J.; Skelton, B. W.; White, A. H.; Wilner, F. R. *Aust. J. Chem.* **1994**, *47*, 143.

Table 2. Atomic Coordinates for $\{[Ni(HN\text{-}Me_6sar)](ClO_4)_3 \cdot 2H_2O\}_3$

atom	x	y	z	atom	x	y	z
Ni(1)	0.1066(3)	0.2060(3)	0.6564(2)	N(303)	0.370(2)	0.474(1)	0.173(1)
Ni(2)	0.2663(4)	0.0636(3)	0.1104(2)	N(306)	0.575(2)	0.351(1)	0.1590(10)
Ni(3)	0.5923(3)	0.4654(3)	0.3166(2)	N(310)	0.704(2)	0.468(1)	0.260(1)
Cl(1)	0.5018(7)	0.1457(5)	0.3328(4)	N(313)	0.509(2)	0.581(1)	0.2642(10)
Cl(2)	0.2593(7)	0.4796(5)	0.5361(4)	N(316)	0.484(2)	0.461(1)	0.3712(9)
Cl(3)	0.2829(7)	0.4375(5)	0.9680(4)	N(319)	0.665(2)	0.346(1)	0.3579(9)
Cl(4)	0.4749(7)	0.1602(5)	0.8662(4)	C(101)	0.048(2)	0.225(2)	0.511(1)
Cl(5)	0.9226(9)	0.2250(6)	0.8183(5)	C(102)	0.146(2)	0.242(2)	0.503(1)
Cl(6)	0.1198(7)	0.4351(5)	0.3124(4)	C(104)	0.308(2)	0.216(2)	0.453(1)
Cl(7)	0.6843(7)	0.2300(6)	0.5966(4)	C(105)	0.360(2)	0.233(2)	0.508(1)
Cl(3)	0.9757(8)	0.1345(6)	0.3243(5)	C(107)	0.421(2)	0.182(2)	0.623(1)
Cl(9)	0.7839(8)	0.1058(6)	0.0930(5)	C(108)	0.336(2)	0.189(2)	0.673(1)
O(1)	0.817(3)	0.049(2)	0.524(2)	C(109)	0.249(2)	0.275(2)	0.647(1)
O(2)	1.004(2)	0.402(1)	0.840(1)	C(111)	0.080(2)	0.374(2)	0.644(1)
O(3)	0.556(2)	0.436(1)	0.9185(9)	C(112)	0.033(2)	0.373(2)	0.585(1)
O(4)	0.638(2)	0.269(1)	0.938(1)	C(114)	−0.036(2)	0.295(2)	0.534(1)
O(5)	0.062(2)	0.369(1)	0.9663(10)	C(115)	0.056(2)	0.136(2)	0.553(1)
O(6)	0.304(2)	0.017(1)	0.5179(9)	C(117)	0.165(2)	0.043(2)	0.646(1)
O(11)	0.557(2)	0.131(2)	0.285(2)	C(118)	0.200(2)	0.034(2)	0.711(1)
O(12)	0.449(2)	0.231(2)	0.322(1)	C(120)	0.311(2)	0.110(2)	0.680(1)
O(13)	0.438(2)	0.103(2)	0.338(1)	C(121)	0.183(3)	0.180(2)	0.409(2)
O(14)	0.554(3)	0.120(2)	0.392(2)	C(122)	0.481(2)	0.093(2)	0.553(1)
O(21)	0.351(2)	0.408(1)	0.5338(10)	C(123)	0.171(2)	0.291(2)	0.746(1)
O(22)	0.265(1)	0.553(1)	0.4960(9)	C(124)	−0.096(2)	0.325(2)	0.633(1)
O(23)	0.172(2)	0.469(1)	0.520(1)	C(125)	−0.014(3)	0.113(2)	0.653(2)
O(24)	0.263(2)	0.481(1)	0.600(1)	C(126)	0.242(3)	0.100(2)	0.784(2)
O(31)	0.277(3)	0.500(2)	0.998(2)	C(201)	0.057(2)	0.129(2)	0.023(1)
O(32)	0.371(3)	0.425(2)	0.938(2)	C(202)	0.019(2)	0.183(2)	0.070(1)
O(33)	0.202(2)	0.466(2)	0.919(1)	C(204)	−0.079(2)	0.315(2)	0.092(1)
O(34)	0.284(2)	0.373(2)	1.016(1)	C(205)	−0.009(2)	0.298(2)	0.152(1)
O(41)	0.500(2)	0.192(1)	0.915(1)	C(207)	0.160(2)	0.272(2)	0.196(1)
O(42)	0.522(2)	0.181(1)	0.810(1)	C(208)	0.248(2)	0.187(2)	0.197(1)
O(43)	0.372(3)	0.197(2)	0.851(1)	C(209)	0.287(2)	0.204(2)	0.130(1)
O(44)	0.504(2)	0.078(2)	0.892(1)	C(211)	0.376(2)	0.158(2)	0.042(1)
O(51)	0.997(3)	0.197(2)	0.776(2)	C(212)	0.283(2)	0.181(2)	−0.002(1)
O(52)	0.901(3)	0.303(3)	0.811(2)	C(214)	0.139(2)	0.145(2)	−0.018(1)
O(53)	0.943(2)	0.169(2)	0.877(1)	C(215)	0.089(2)	0.037(2)	0.058(1)
O(54)	0.837(3)	0.223(2)	0.788(2)	C(217)	0.128(2)	−0.003(2)	0.172(1)
O(61)	0.210(2)	0.371(2)	0.302(1)	C(218)	0.210(2)	−0.023(2)	0.224(1)
O(62)	0.141(2)	0.509(2)	0.304(1)	C(220)	0.207(2)	0.118(2)	0.217(1)
O(63)	0.085(2)	0.411(2)	0.372(1)	C(221)	−0.110(2)	0.300(2)	−0.011(1)
O(64)	0.041(2)	0.451(2)	0.267(1)	C(222)	0.070(2)	0.397(2)	0.114(1)
O(71)	0.590(2)	0.285(2)	0.567(1)	C(223)	0.454(3)	0.092(2)	0.148(2)
O(72)	0.684(2)	0.153(2)	0.622(1)	C(224)	0.311(2)	0.041(2)	−0.014(1)
O(73)	0.714(2)	0.252(2)	0.648(1)	C(225)	0.240(2)	−0.087(2)	0.108(1)
O(74)	0.761(2)	0.221(1)	0.552(1)	C(226)	0.366(3)	−0.008(2)	0.251(2)
O(81)	0.890(3)	0.130(2)	0.346(1)	C(301)	0.355(2)	0.538(2)	0.269(1)
O(82)	0.983(1)	0.214(1)	0.3140(9)	C(302)	0.394(2)	0.458(2)	0.245(1)
O(83)	1.068(2)	0.072(2)	0.345(1)	C(304)	0.384(2)	0.390(2)	0.159(1)
O(84)	0.958(3)	0.123(2)	0.259(2)	C(305)	0.490(2)	0.325(2)	0.178(1)
O(91)	0.686(2)	0.109(2)	0.102(1)	C(307)	0.673(2)	0.294(2)	0.193(1)
O(92)	0.826(3)	0.132(2)	0.132(2)	C(308)	0.708(2)	0.328(2)	0.245(1)
O(93)	0.849(2)	0.022(2)	0.099(1)	C(309)	0.690(2)	0.420(2)	0.214(1)
O(94)	0.788(3)	0.148(2)	0.031(2)	C(311)	0.674(2)	0.558(2)	0.225(1)
N(103)	0.226(2)	0.186(1)	0.468(1)	C(312)	0.567(2)	0.596(2)	0.207(1)
N(106)	0.394(2)	0.161(1)	0.564(1)	C(314)	0.399(2)	0.601(2)	0.242(1)
N(110)	0.155(2)	0.288(1)	0.680(1)	C(315)	0.372(2)	0.514(2)	0.344(1)
N(113)	−0.002(2)	0.302(1)	0.598(1)	C(317)	0.495(2)	0.371(2)	0.392(1)
N(116)	0.075(2)	0.123(1)	0.623(1)	C(318)	0.604(2)	0.317(1)	0.411(1)
N(119)	0.218(2)	0.110(1)	0.7140(10)	C(320)	0.660(2)	0.302(2)	0.307(1)
N(203)	−0.028(2)	0.276(1)	0.042(1)	C(321)	0.260(3)	0.527(2)	0.152(2)
N(206)	0.087(2)	0.310(1)	0.1395(10)	C(322)	0.575(2)	0.365(2)	0.088(1)
N(210)	0.354(2)	0.129(1)	0.111(1)	C(323)	0.815(2)	0.435(2)	0.285(1)
N(213)	0.247(2)	0.111(1)	0.0149(10)	C(324)	0.511(2)	0.640(2)	0.303(1)
N(216)	0.177(2)	0.004(1)	0.1098(10)	C(325)	0.502(2)	0.485(2)	0.429(1)
N(219)	0.265(2)	0.036(1)	0.2047(10)	C(326)	0.771(2)	0.308(2)	0.392(1)

a BAS 100 electrochemical analyzer employing glassy carbon working, platinum counter and saturated calomel reference electrodes. A mercury pool was employed as the working electrode for bulk electrolysis experiments. All solutions were 1−5 mM in analyte and 0.1 M in $NaClO_4$. Each solution was measured at ambient temperature and purged with nitrogen. Molecular mechanics calculations were performed with the strain energy minimization program MOMEC87[11] using published force fields.[12]

Structure Analyses. Intensity data for all compounds were measured on a Rigaku AFC6R diffractometer using graphite monochromated Cu Kα radiation (λ=1.54178 Å). Data were collected at

(10) Martinelli, R. A.; Hanson, G. R.; Thompson, J. S.; Holmquist, B.; Pilbrow, J. R.; Auld, D. S.; Vallee, B. L. *Biochemistry* **1989**, *28*, 2251.

Table 3. Atomic Coordinates for $[Ni(N\text{-}Me_5sar)](ClO_4)_2$

atom	x	y	z
Ni	0.2700(2)	0.1132(1)	0.15680(5)
Cl(1)	0.2684(4)	0.1007(3)	0.90817(9)
Cl(2)	0.7461(3)	0.0410(2)	0.77564(8)
O(11)	0.158(1)	0.0263(10)	0.9019(4)
O(12)	0.362(1)	0.0407(9)	0.9390(3)
O(13)	0.2309(9)	0.2134(6)	0.9351(2)
O(14)	0.3259(10)	0.1313(7)	0.8598(2)
O(21)	0.6314(6)	0.0441(7)	0.8100(2)
O(22)	0.7919(8)	−0.0849(5)	0.7707(2)
O(23)	0.8524(7)	0.1165(7)	0.7969(3)
O(24)	0.7084(7)	0.0859(5)	0.7246(2)
N(3)	−0.0092(10)	−0.1303(8)	0.0733(3)
N(6)	0.291(1)	−0.2435(7)	0.0892(3)
N(10)	0.2700(9)	0.0287(6)	0.2262(2)
N(13)	0.0876(7)	0.1650(6)	0.1704(2)
N(16)	0.2559(9)	0.1876(6)	0.0864(2)
N(19)	0.4499(7)	0.0545(7)	0.1373(3)
C(1)	0.014(1)	0.104(1)	0.0784(4)
C(2)	−0.059(1)	−0.009(1)	0.0531(4)
C(4)	0.077(1)	−0.1998(10)	0.0372(4)
C(5)	0.172(1)	−0.2941(10)	0.0632(4)
C(7)	0.254(1)	−0.1887(7)	0.1405(3)
C(8)	0.3742(10)	−0.1528(8)	0.1766(3)
C(9)	0.3293(9)	−0.0996(8)	0.2288(3)
C(11)	0.1234(9)	0.0228(9)	0.2417(3)
C(12)	0.0567(9)	0.1426(9)	0.2269(3)
C(14)	−0.0076(8)	0.0931(10)	0.1374(3)
C(15)	0.160(1)	0.1018(9)	0.0597(3)
C(17)	0.390(1)	0.179(1)	0.0615(3)
C(18)	0.458(1)	0.059(1)	0.0780(4)
C(20)	0.490(1)	−0.0763(9)	0.1536(4)
C(21)	−0.122(1)	−0.207(1)	0.0930(5)
C(22)	0.388(1)	−0.3486(9)	0.0958(4)
C(23)	0.3418(9)	0.1067(9)	0.2660(3)
C(24)	0.211(1)	0.3205(9)	0.0804(3)
C(25)	0.553(1)	0.145(1)	0.1573(4)

room temperature, except where noted. For $\{[Ni(HN\text{-}Me_6sar)](ClO_4)_3{\cdot}2H_2O\}_3$ severe crystal decay necessitated collection at low temperature. The $\omega/2\theta$ scan technique was employed throughout with variable scan speeds in the 2θ range of 3−120°. For each structure, the intensities of three standard reflections were measured periodically, and corrections applied where necessary. Data were also corrected for Lorentz/polarization effects and absorption, based on the azimuthal (Ψ) scans of reflections of Eulerian angle χ near 90°.[13] The structures were solved by heavy atom Patterson methods[14] and expanded using Fourier techniques.[15] All non-hydrogen atoms were refined anisotropically (except in the case of $\{[Ni(HN\text{-}Me_6sar)](ClO_4)_3{\cdot}2H_2O\}_3$ where the relatively small number of observed reflections could only support anisotropic thermal parameters for the Ni and Cl atoms) by full matrix least squares methods to minimize the function $\Sigma w(F_o - F_c)^2$, where $w^{-1} = \sigma^2(F) + p(F)^2$. Hydrogen atoms were included in the calculations at known positions with fixed C−H bonding distances of 0.96 Å. Chiralities for the noncentrosymmetric structures were assigned on the basis of refinements in each enantiomorph. Atomic scattering factors for neutral atoms were taken from the literature,[16] and anomalous dispersion effects were included in Fcalc.[17] The values of $\Delta f'$ and f''[18] and the mass attenuation coefficients[19] were taken from the literature. All calculations were performed with the teXsan crystallographic package.[20] Drawings of all molecules were produced with the plotting program CHARON.[20] Non-hydrogen positional parameters for all structures are listed in Tables 2−6.

Table 4. Atomic Coordinates for $[Ni(N\text{-}Me_7sar)](ClO_4)_3$

atom	x	y	z
Ni(1)	0.7623(1)	0.91075(7)	0.81451(4)
Cl(1)	0.2642(2)	0.7119(1)	0.91455(8)
Cl(2)	0.2468(2)	0.8705(1)	0.66168(8)
Cl(3)	0.7549(2)	0.6913(1)	0.64529(8)
O(11)	0.236(1)	0.7699(5)	0.9646(2)
O(12)	0.1642(5)	0.6470(5)	0.9021(3)
O(13)	0.2848(5)	0.7719(4)	0.8617(2)
O(14)	0.3722(5)	0.6562(5)	0.9298(3)
O(21)	0.2623(7)	0.8632(6)	0.7259(3)
O(22)	0.1204(5)	0.8513(5)	0.6500(3)
O(23)	0.3219(6)	0.7955(5)	0.6342(3)
O(24)	0.2845(7)	0.9628(4)	0.6407(4)
O(31)	0.7741(6)	0.6098(4)	0.6856(3)
O(32)	0.6283(4)	0.7187(4)	0.6440(2)
O(33)	0.7910(7)	0.6706(5)	0.5846(3)
O(34)	0.8270(6)	0.7725(5)	0.6672(3)
N(3)	0.5842(5)	1.0161(4)	0.9862(2)
N(6)	0.8832(6)	1.0954(4)	0.9979(2)
N(10)	0.9095(5)	0.8463(4)	0.8497(2)
N(13)	0.6615(5)	0.8026(4)	0.8506(2)
N(16)	0.6144(5)	0.9773(4)	0.7811(2)
N(19)	0.8610(5)	1.0251(4)	0.7854(2)
C(1)	0.5113(6)	0.9436(5)	0.8848(3)
C(2)	0.5578(7)	1.0340(5)	0.9215(3)
C(4)	0.6427(7)	1.1036(5)	1.0165(3)
C(5)	0.7724(7)	1.0845(5)	1.0418(3)
C(7)	0.8788(7)	1.0101(5)	0.9516(3)
C(8)	0.9648(6)	1.0173(5)	0.8949(3)
C(9)	1.0100(6)	0.9128(5)	0.8748(3)
C(11)	0.8643(7)	0.7820(5)	0.9012(3)
C(12)	0.7499(8)	0.7281(4)	0.8793(3)
C(14)	0.5850(6)	0.8472(5)	0.9016(3)
C(15)	0.4951(6)	0.9664(6)	0.8160(3)
C(17)	0.6478(7)	1.0860(5)	0.7766(3)
C(18)	0.7758(7)	1.0958(5)	0.7519(3)
C(20)	0.9110(6)	1.0809(5)	0.8416(3)
C(21)	0.4725(8)	0.9858(6)	1.0194(3)
C(22)	0.9996(7)	1.0859(7)	1.0356(3)
C(23)	0.9688(7)	0.7783(5)	0.8026(3)
C(24)	0.5818(7)	0.7418(5)	0.8088(4)
C(25)	0.5912(7)	0.9417(5)	0.7156(3)
C(26)	0.9637(8)	1.0020(5)	0.7413(3)
C(27)	0.8829(10)	1.1975(5)	0.9686(3)

Results

Nickel(II) Complexes. Complexation of nickel(II) with each of the N-methylated, hexaaza macrocycles proved to be relatively straightforward. The rather long reaction times were found to be necessary as complex formation was rather slow by comparison with acyclic and non-methylated secondary amine relatives. It is unlikely that the poor solubility of the ligand in water had a detrimental effect on reaction rate, as parallel reactions in methanol, in which the reactants are very soluble, did not result in an appreciable increase in the rate of complex formation. Separation of the dipositively charged complexes $[Ni(N\text{-}Me_5sar)]^{2+}$ and $[Ni(N\text{-}Me_6sar)]^{2+}$ was achieved

(11) Hambley, T. W. MOMEC87, a FORTRAN program for Strain Energy Minimization. University of Sydney, Australia, 1987.
(12) Bernhardt, P. V.; Comba, P.; Hambley, T. W. *Inorg. Chem.* **1993**, *32*, 2804.
(13) North, A. C. T.; Phillips, D. C.; Mathews, F. S. *Acta Crystallogr.*, **1968**, *A24*, 351.
(14) Beurskens, P. T.; Admiraal, G.; Beurskens, G.; Bosman, W. P.; Garcia-Granda, S.; Gould, R. O.; Smits, J. M. M.; Smykalla, C. PATTY: The DIRDIF Program System. Technical Report of the Crystallography Laboratory, University of Nijmegen, The Netherlands, 1992.
(15) Beurskens, P. T.; Admiraal, G.; Beurskens, G.; Bosman, W. P.; Garcia-Granda, S.; Gould, R. O.; Smits, J. M. M.; Smykalla, C. DIRDIF92: The DIRDIF Program System. Technical Report of the Crystallography Laboratory, University of Nijmegen, The Netherlands, 1992.
(16) Cromer, D. T.; Waber, J. T. *International Tables for X-ray Crystallography*; The Kynoch Press: Birmingham, England, Table 2.2A, 1974; Vol. IV.
(17) Ibers, J. A.; Hamilton, W. C. *Acta Crystallogr.* **1964**, *17*, 781.
(18) Creagh, D. C.; McAuley, W. J. *International Tables for Crystallography*; (Wilson, A. J. C., Ed.; Kluwer Academic Publishers: Boston, 1992; Vol. C, Table 4.2.6.8, pp 219−222.
(19) Creagh, D. C.; Hubbell, J. H. *International Tables for Crystallography*; Wilson, A. J. C., Ed.; Kluwer Academic Publishers: Boston, 1992; Vol. C, Table 4.2.4.3, pp 200−206.
(20) teXsan: Single Crystal Structure Analysis Software, Version 1.6c; Molecular Structure Corp.: The Woodlands, TX, 1993.

Table 5. Atomic Coordinates for $[Cu(N\text{-}Me_5sar)](ClO_4)_2$

atom	x	y	z
Cu(1)	0.22925(8)	0.36420(8)	0.33947(3)
Cl(1)	0.2484(2)	0.0476(1)	0.28156(6)
Cl(2)	−0.2243(2)	−0.0989(2)	−0.08896(7)
O(11)	0.1672(4)	0.1493(4)	0.3022(2)
O(12)	0.3607(4)	0.0269(5)	0.3151(2)
O(13)	0.1717(5)	−0.0648(4)	0.2784(2)
O(14)	0.2937(4)	0.0821(4)	0.2304(1)
O(21)	−0.2606(6)	−0.2171(4)	−0.0653(1)
O(22)	−0.1633(5)	−0.1261(6)	−0.1383(2)
O(23)	−0.3345(6)	−0.0239(6)	−0.0956(2)
O(24)	−0.1297(7)	−0.0375(6)	−0.0568(2)
N(3)	0.4953(6)	0.6293(6)	0.4281(2)
N(6)	0.1930(6)	0.7301(5)	0.4084(2)
N(10)	0.2361(5)	0.4631(4)	0.2692(2)
N(13)	0.4239(5)	0.3262(5)	0.3293(2)
N(16)	0.2438(5)	0.2963(4)	0.4145(2)
N(19)	0.0435(5)	0.4268(5)	0.3592(2)
C(1)	0.4787(6)	0.3935(7)	0.4227(3)
C(2)	0.5447(7)	0.5092(7)	0.4487(3)
C(4)	0.4055(8)	0.6987(7)	0.4622(3)
C(5)	0.3070(9)	0.7878(7)	0.4355(3)
C(7)	0.2351(7)	0.6773(5)	0.3575(2)
C(8)	0.1212(6)	0.6403(6)	0.3204(2)
C(9)	0.1719(6)	0.5915(6)	0.2689(2)

Table 6. Atomic Coordinates for $[Cu(N\text{-}Me_7sar)](ClO_4)_3{\cdot}0.5H_2O$

atom	x	y	z
Cu	0.2230(2)	0.1242(1)	0.19393(7)
Cl(1)	0.2037(4)	0.2700(3)	0.3356(1)
Cl(2)	0.7497(3)	0.2643(3)	0.0856(2)
Cl(3)	0.2083(4)	0.3853(3)	0.6443(2)
O(1)*	0.178(3)	0.432(5)	0.481(1)
O(11)	0.1850(9)	0.2015(8)	0.2845(4)
O(12)	0.224(1)	0.3745(8)	0.3111(5)
O(13)	0.3081(9)	0.2342(8)	0.3690(4)
O(14)	0.1035(10)	0.268(1)	0.3737(5)
O(21)	0.6287(8)	0.2922(10)	0.0696(5)
O(22)	0.789(1)	0.190(1)	0.0456(5)
O(23)	0.820(1)	0.359(1)	0.0839(9)
O(24)	0.756(1)	0.226(1)	0.1435(5)
O(31)	0.252(2)	0.429(1)	0.5975(9)
O(32)	0.278(2)	0.301(1)	0.6621(7)
O(33)	0.185(2)	0.4546(10)	0.6944(8)
O(34)	0.101(2)	0.337(2)	0.6333(8)
N(3)	0.1644(10)	−0.0672(9)	0.0119(5)
N(6)	0.448(1)	−0.0359(9)	0.0519(5)
N(10)	0.3844(9)	0.1904(8)	0.1835(4)
N(13)	0.1642(9)	0.2331(8)	0.1330(5)
N(16)	0.0665(10)	0.0406(8)	0.1887(5)
N(19)	0.2952(10)	−0.0082(8)	0.2344(4)
C(1)	0.064(1)	0.0847(10)	0.0753(6)
C(2)	0.178(1)	0.030(1)	0.0513(5)
C(4)	0.282(2)	−0.098(1)	−0.0148(6)
C(5)	0.382(2)	−0.127(1)	0.0288(6)
C(7)	0.520(1)	−0.058(1)	0.1052(6)
C(8)	0.471(1)	0.002(1)	0.1627(7)
C(9)	0.449(1)	0.116(1)	0.1402(5)
C(11)	0.367(1)	0.292(1)	0.1514(6)
C(12)	0.273(1)	0.2811(10)	0.1045(5)
C(14)	0.083(1)	0.1997(10)	0.0830(6)
C(15)	0.002(1)	0.040(1)	0.1300(6)
C(17)	0.099(1)	−0.072(1)	0.2021(7)
C(18)	0.189(1)	−0.077(1)	0.2486(6)
C(20)	0.364(1)	−0.060(1)	0.1860(7)
C(21)	0.086(1)	−0.045(1)	−0.0414(6)
C(22)	0.521(2)	0.013(2)	0.0033(7)
C(23)	0.466(1)	0.215(1)	0.2350(6)
C(24)	0.102(1)	0.322(1)	0.1662(7)
C(25)	−0.018(1)	0.075(1)	0.2357(6)
C(26)	0.362(1)	−0.004(1)	0.2914(5)
C(27)	0.114(2)	−0.163(1)	0.0437(8)

by ion-exchange chromatography with Na_2HPO_4 solution as the eluent, whereas NaCl or $NaClO_4$ solutions did not afford separation of these two species. The tripositive $[Ni(N\text{-}Me_7sar)]^{3+}$ ion eluted well behind the other two regardless of the eluent. All three Ni(II) complexes were crystallized as their perchlorate salts and each was characterized structurally by X-ray analysis.

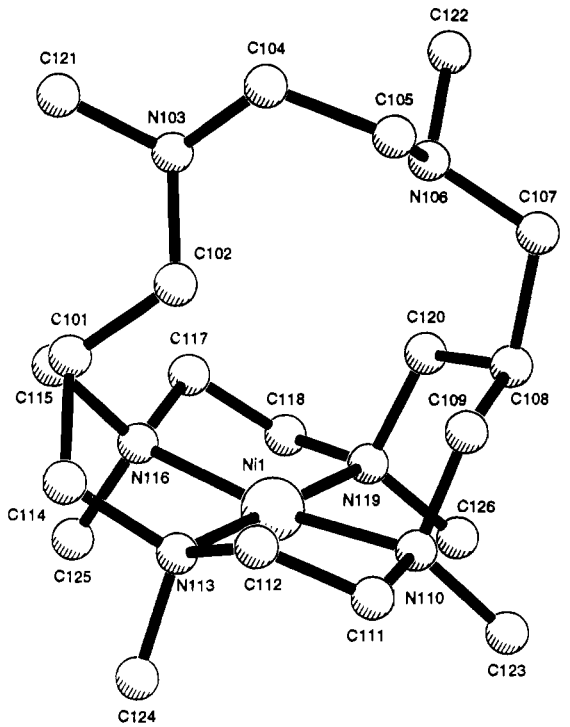

Figure 1. Drawing of $[Ni(HN\text{-}Me_6sar)]^{3+}$ (cation 1).

For the protonated complex $[Ni(HN\text{-}Me_6sar)](ClO_4)_3{\cdot}2H_2O$, the X-ray structure determination revealed that the molecule crystallizes in a trimeric array consisting of three crystallographically independent complex cations, nine perchlorate anions and six water molecules all at general sites, with an extensive network of H-bonding stabilizing this rather unusual structure. A drawing of one of the $[Ni(HN\text{-}Me_6sar)]^{3+}$ cations (cation 1) is shown in Figure 1. There are no major differences between the three crystallographically distinct $[Ni(HN\text{-}Me_6sar)]^{3+}$ cations, although one of the free tertiary amines (N(306) in cation 3) is inverted in relation to the corresponding amines in the other two cations. Selected bond lengths and angles are assembled in Table 7. There are several notable features concerning the geometry of the complex cation. Firstly, the ligand only coordinates as a tetradentate and the configuration of the four coordinated amines is *R,S,R,S,* which is commonly referred to as *trans-I*,[21] where the four methyl groups lie on the same side of the NiN_4 plane. There is a significant deviation (0.09(2) Å) of the Ni-atom from the least-squares plane of four N-donors away from the noncoordinated diamine strap, and also a tetrahedral distortion of the array of coordinated N-atoms (0.08(2) Å deviation of the N-atoms from the plane). Nevertheless, the environment of the metal center is essentially square-planar, where the closest intermolecular contact with the Ni-atom is 3.01(4) Å (Ni(1)-O(51)). The conformation of the ligand also deserves some comment. Inspection of Figure 1 reveals that the two five-membered chelate rings have opposite chiralities, i.e. they adopt an eclipsed arrangement. The conformations of the two six-membered chelate rings are different; the ring containing N(a10) and N(a19) (a = 1,2 or 3) adopts a chair conformation while the opposite ring assumes a less stable boat conformation. The Ni−N bond lengths are

(21) Bosnich, B.; Poon, C. K.; Tobe, M. L. *Inorg. Chem.* **1965**, *4*, 1106.

Table 7. Selected Bond Lengths (Å) and Angles (deg)

	$[Ni(N\text{-}Me_5sar)]^{2+}$	$[Ni(HN\text{-}Me_6sar)]^{3+}$[a]	$[Ni(N\text{-}Me_7sar)]^{3+}$	$[Cu(N\text{-}Me_5sar)(OClO_3)]^{+}$	$[Cu(N\text{-}Me_7sar)(OClO_3)]^{2+}$
M−N(10)	1.990(6)	2.00(2)	1.957(5)	2.0884(4)	2.029(11)
M−N(13)	1.923(7)	1.96(2)	1.972(5)	2.005(5)	2.052(10)
M−N(16)	1.970(6)	1.98(2)	1.962(6)	2.063(4)	2.075(11)
M−N(19)	1.956(8)	1.97(2)	1.968(5)	2.036(5)	2.086(10)
M−O(11)				2.534(5)	2.280(9)
N(10)−M−N(13)	88.2(3)	87.8(9)	88.0(2)	87.4(2)	86.2(4)
N(10)−M−N(16)	174.9(4)	170.8(9)	178.6(2)	168.7(2)	168.4(4)
N(10)−M−N(19)	94.7(3)	91.3(9)	91.9(2)	94.8(2)	92.0(4)
O(11)−M−N(10)				97.2(2)	95.2(4)
O(11)−M−N(13)				90.6(2)	103.0(4)
M−N(10)−C(11)	104.7(5)	105(1)	106.4(4)	103.2(3)	107.5(8)
M−N(10)−C(9)	117.2(5)	101(1)	117.4(4)	116.1(3)	104.1(7)
M−N(13)−C(12)	108.8(5)	106(1)	107.7(4)	106.7(3)	106.6(6)
M−N(13)−C(14)	110.2(5)	119(1)	107.4(4)	110.1(4)	119.4(8)

[a] Data for Cation 1 only.

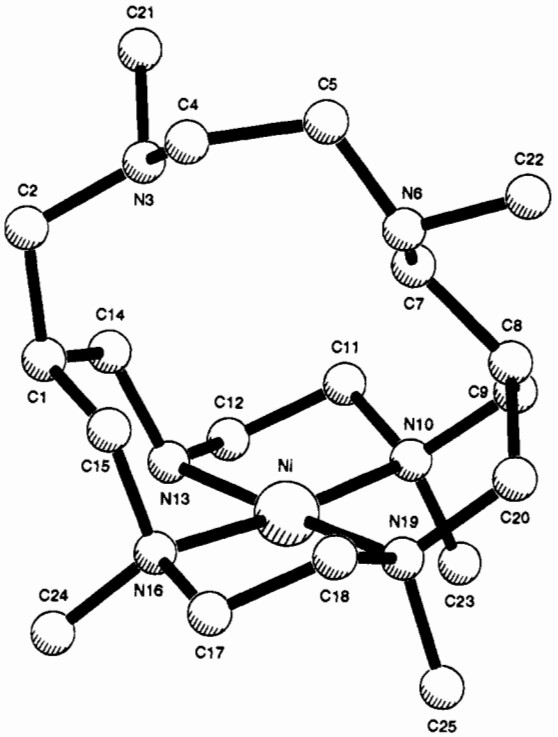

Figure 2. Drawing of $[Ni(N\text{-}Me_5sar)]^{2+}$.

consistent with a low-spin d^8 ground state of Ni(II), although they are somewhat longer than those found in tetra-aminenickel-(II) complexes bearing secondary amines.[22,23] The extension of the Ni−N bond upon N-methylation is clearly a result of steric repulsion between the methyl group and the ligand backbone.

The structural analysis of $[Ni(N\text{-}Me_5sar)](ClO_4)_2$ found the complex cation and two anions to be situated at general positions. Inspection of Figure 2 shows that the sole secondary amine (N(13)) is coordinated, and that it exhibits a significantly shorter Ni−N bond length (Table 7) than the remaining three coordinated, tertiary amines. The configuration of the four N-donors and the conformation of $[Ni(N\text{-}Me_5sar)]^{2+}$ is the same as that found in the structure of $[Ni(HN\text{-}Me_6sar)](ClO_4)_3\cdot 2H_2O$. The deviation of the metal center from the least squares N_4 plane away from the noncoordinated strap (0.07 Å) is the same within experimental error, and the closest axial interaction with the Ni-atom is 3.228(7) Å to O(23). However, there is no significant deviation of the four N-donors from the least-squares N_4 plane in $[Ni(N\text{-}Me_5sar)]^{2+}$.

The ^1H NMR spectrum of $[Ni(N\text{-}Me_5sar)]^{2+}$ in D_2O was consistent with its asymmetry, with five distinct singlet methyl resonances at 2.24, 2.46, 2.60, 3.16 and 3.22 ppm. On the whole, the linewidths were rather broad as a result of unresolved H-H coupling and the presence of some of the high-spin form of the complex (see below), and no assignment of H-H coupling could be made. The H-decoupled ^{13}C NMR spectrum of $[Ni(N\text{-}Me_5sar)]^{2+}$ yielded fourteen of the anticipated nineteen resonances, with several broad and intense resonances being indicative of accidental degeneracies. The NMR spectra of $[Ni(N\text{-}Me_6sar)]^{2+}$ and $[Ni(N\text{-}Me_7sar)]^{3+}$ were not measured as they exhibited quite strong paramagnetism in both protic and aprotic solvents. Although the paramagnetically shifted ^1H NMR spectra of high-spin Ni(II) complexes are known,[24] H-H coupling is generally not resolved, so a study of this type was not pursued for $[Ni(N\text{-}Me_6sar)]^{2+}$ or $[Ni(N\text{-}Me_7sar)]^{3+}$.

The structure of $[Ni(N\text{-}Me_7sar)](ClO_4)_3\cdot H_2O$ once again revealed that the *trans-I* configuration of the N-donors was present and a drawing of the complex cation is given in Figure 3. A square-planar geometry, with a tetrahedral distortion (0.032(5) Å), of the NiN_4 chromophore is defined with the Ni-atom deviating 0.057 Å from the least-squares plane of N-donors away from the noncoordinated strap. There are no intermolecular contacts to the Ni-atom within 3.6 Å. The average Ni−N bond lengths in $[Ni(HN\text{-}Me_6sar)]^{3+}$ and $[Ni(N\text{-}Me_7sar)]^{3+}$ (Table 7) do not differ significantly. However, the conformations of the ligands in the two complexes are quite different. In the $[Ni(N\text{-}Me_7sar)]^{3+}$ cation, both six-membered chelate rings adopt skew-boat conformations and the two five-membered chelate rings have like chiralities (a staggered arrangement).

The solution electronic spectra of the Ni(II) complexes exhibited marked temperature, solvent and pH dependencies. The origin of these observations lies in the solvent dependent high-spin/low-spin equilibrium between the triplet and singlet d^8 electronic ground states of the two forms (eq 1), where S

$$\underset{\text{(low-spin)}}{[Ni^{II}L]^{m+}} + nS \overset{K}{\rightleftharpoons} \underset{\text{(high-spin)}}{[Ni^{II}L(S)_n]^{m+}} \qquad (1)$$

represents the solvent and n = 1 or 2.[24-27] The electronic spectra of $[Ni(N\text{-}Me_6sar)]^{2+}$ and $[Ni(N\text{-}Me_5sar)]^{2+}$ in water,

(22) McAuley, A.; Subramanian, S. *Inorg. Chem.* **1991**, *30*, 371.
(23) Fabbrizzi, L.; Manotti Lanfredi, A. M.; Pallavicini, P.; Perotti, A.; Taglietti, A.; Ugozzoli, F. *J. Chem. Soc., Dalton Trans.* **1991**, 3263.
(24) Herron, N.; Moore, P. *Inorg. Chim. Acta* **1979**, *36*, 89.
(25) Iwamoto, E.; Yokoyama, T.; Yamasaki, S.; Yabe, T.; Kumumaru, T.; Yamamoto, Y. *J. Chem. Soc., Dalton Trans.* **1988**, 1935.
(26) Sabatini, L.; Fabbrizzi, L. *Inorg. Chem.* **1979**, *89*, 438.
(27) Lincoln, S. F.; Hambley, T. W.; Pisaniello, D. L.; Coates, J. H. *Aust. J. Chem.* **1984**, *37*, 713.

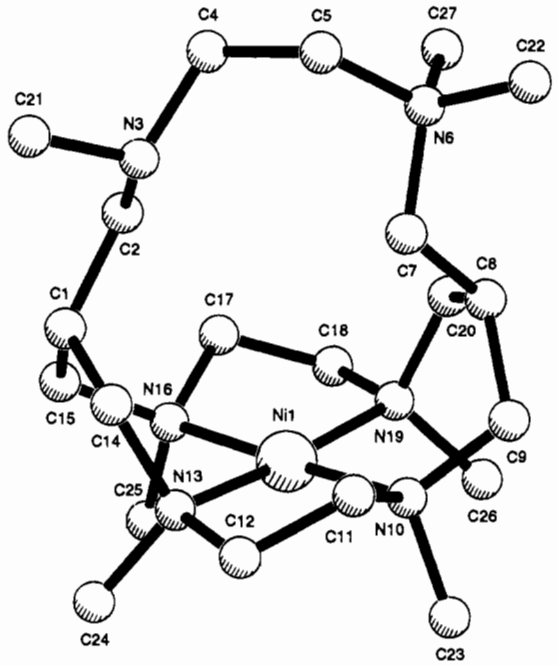

Figure 3. Drawing of $[Ni(N\text{-}Me_7sar)]^{3+}$.

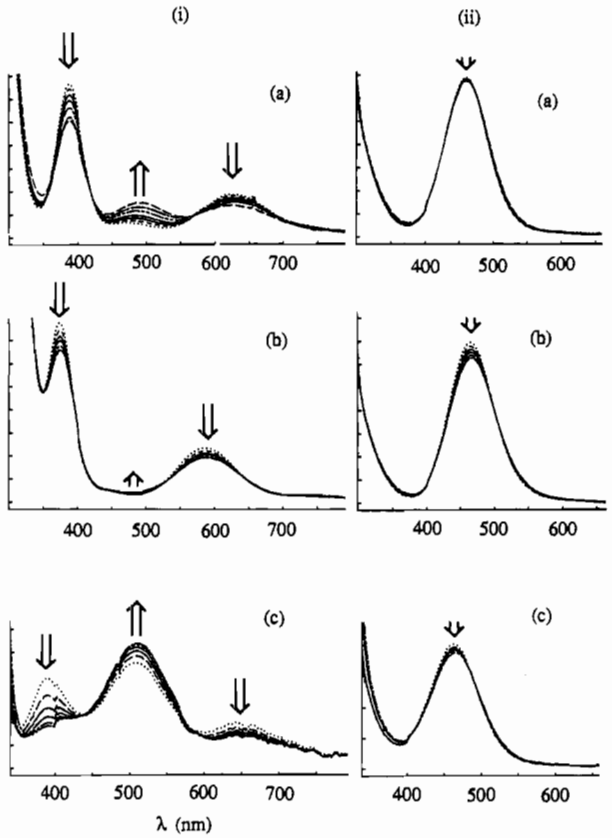

Figure 4. Electronic spectra of (i) $[Ni(N\text{-}Me_6sar)]^{2+}$ and (ii) $[Ni(N\text{-}Me_5sar)]^{2+}$ in (a) water, (b) acetonitrile and (c) acetone. Key: (••) 288 K; (- - -) 298 K; (—) 308 K; (— - - —) 318 K; (— - —) 328 K; (— —) 338 K. (arbitrary absorbance scale).

acetonitrile and acetone as a function of temperature are shown in Figure 4, and the data for all three complexes are reported in Table 8. The spectra of $[Ni(N\text{-}Me_6sar)]^{2+}$ and $[Ni(N\text{-}Me_7sar)]^{3+}$ were essentially the same and exhibited well-defined isosbestic points, indicating that the equilibria each involve only one process and almost certainly only two absorbing species. The lowest and highest energy visible transitions at ~580 (one component of $^3T_{1g} \leftarrow {}^3A_{2g}$ (O_h)) and ~380 nm ($^3T_{2g} \leftarrow {}^3A_{2g}$ (O_h)) were due to the solvated, square-pyramidal, high-spin adduct whereas the maxima between 460–500 nm (($^1A_{2g} \leftarrow {}^1A_{1g}$ (D_{4h})) were characteristic of the low-spin, square-planar form of each complex. The energy of the two high-spin transitions were strongly dependent on the solvent, with a bathochromic shift resulting on going from acetone to water to acetonitrile. This is consistent with the expected donor strengths of the three ligands. Assuming that the equilibria involved in these processes are represented by Eqn 1, $\Delta H°$ and $\Delta S°$ may be determined from a plot of $-\ln K$ vs $1/T$ and these values are listed in Table 8. Generally, it has been found that the low-spin form of tetra-azamacrocyclic nickel(II) complexes may be stabilized, to the exclusion of the high-spin form, with high concentrations of electrolyte.[23] However, in this instance, the spectrum of $[Ni(N\text{-}Me_6sar)]^{2+}$ in 6 M $NaClO_4$ still exhibited maxima due to the high-spin form of the complex. The molar absorption coefficients of the pure high- and low-spin forms of each complex were determined by plotting the absorbance for the high spin form ($A_{h.s.}$) versus that of the low spin form ($A_{l.s.}$). It can be shown that these absorbances are related to the molar absorption coefficients ($\epsilon_{h.s.}$ and $\epsilon_{l.s.}$) and total concentration of Ni^{II} ($[Ni]_{tot}$) by eq 2. Therefore, the intercept of this plot yields

$$A_{h.s.} = \epsilon_{h.s.}[Ni]_{tot} - \epsilon_{h.s.}A_{l.s.}/\epsilon_{l.s.} \quad (2)$$

$\epsilon_{h.s.}$ and the slope gives the other molar absorption coefficient. These values are also given in Table 8 with their uncertainties as a result of the extrapolation. There was little variation in the spectra of $[Ni(N\text{-}Me_5sar)]^{2+}$ with either solvent or temperature and no thermodynamic data could be determined. Similarly, variations of the absorbance values for the low-spin forms of $[Ni(N\text{-}Me_6sar)]^{2+}$ and $[Ni(N\text{-}Me_7sar)]^{3+}$ in acetonitrile as a function of temperature were too small to allow accurate determinations of the molar absorption coefficients, and the values given in Table 8 for these complexes represent upper bounds only. Consequently, no thermodynamic data are given for these systems.

Potentiometric and spectrophotometric titrations of the three Ni(II) complexes were also undertaken, and the pK_a values are given in Table 8. For $[Ni(N\text{-}Me_5sar)]^{2+}$ and $[Ni(N\text{-}Me_6sar)]^{2+}$, the higher pK_a value was due to deprotonation of the aqua ligand in the high-spin form of the complex, whereas the other protonation constant was assigned to one of the noncoordinated tertiary amines. These assignments were based on the solution electronic spectra of each complex at various pH values. It was found that the spectra of $[Ni(N\text{-}Me_5sar)]^{2+}$ and $[Ni(N\text{-}Me_6sar)]^{2+}$ were essentially unchanged within the range $2 < pH < 9$. By contrast, at pH 11.5 there was a hypsochromic shift of the two high-spin transitions of $[Ni(N\text{-}Me_6sar)]^{2+}$ from 388 to 417 nm and from 628 to 690 nm, which is consistent with deprotonation of the aqua ligand to give the weaker ligand field hydroxy group. For $[Ni(N\text{-}Me_5sar)]^{2+}$, there was a less dramatic change at pH 11.5, however the low-spin transition was significantly bleached with concomitant growth of maxima at *ca.* 400 and 650 nm. This is consistent with deprotonation of the high-spin adduct $[Ni(N\text{-}Me_5sar)(OH_2)]^{2+}$. The single pK_a value for $[Ni(N\text{-}Me_7sar)(OH_2)]^{3+}$ was unequivocally assigned to an aqua/hydroxy ligand interconversion as the electronic spectrum at pH 9.5 yielded maxima at 416 and 700 nm (*cf* $[Ni(N\text{-}Me_6sar)(OH_2)]^{2+}$ and data in Table 8). Note that the pK_a of the aqua ligand in $[Ni(N\text{-}Me_7sar)]^{3+}$ is much lower than those in $[Ni(N\text{-}Me_5sar)]^{2+}$ and $[Ni(N\text{-}Me_6sar)]^{2+}$; a consequence of the higher charge of the complex cation. The pK_a value of the sole free amine in $[Ni(N\text{-}Me_7sar)]^{3+}$ was too low to be determined potentiometrically.

Table 8. Electronic Spectra[a] and Thermodynamic Data

	pK_a	high spin[a]	low spin	$\Delta H°$, kJ mol^{-1}	$\Delta S°$, J K^{-1} mol^{-1}	n
$[Ni(N\text{-}Me_5sar)]^{2+}$	5.3(1), 10.6(1)		ϵ_{460nm} 63[b]	...	...	...
MeCN			ϵ_{466nm} 68[b]	...	...	...
Me_2CO			ϵ_{468nm} 68[b]	...	...	...
$[Ni(N\text{-}Me_6sar)]^{2+}$	5.3(1), 9.7(1)	ϵ_{388nm} 163(2), ϵ_{628nm} 45(2)	ϵ_{486nm} 108(2)	−16(1)	−40(1)	1
MeCN		ϵ_{374nm} ~250,[c] ϵ_{588nm} ~75[c]	...	...		1
Me_2CO		ϵ_{390nm} 254(4), ϵ_{644nm} 132(2)	ϵ_{508nm} 105(2)	−15(1)	−61(3)	1
$[Ni(N\text{-}Me_7sar)]^{3+}$	6.9(1)	ϵ_{388nm} 191(1), ϵ_{630nm} 57(1)	ϵ_{474nm} 85(1)	−15(1)	−44(1)	1
MeCN		ϵ_{376nm} ~250,[c] ϵ_{586nm} ~75[c]	...	...		1
$[Cu(N\text{-}Me_5sar)]^{2+}$	5.0(1)	ϵ_{282nm} 6210, ϵ_{554nm} 242				
$[Cu(N\text{-}Me_6sar)]^{2+}$	6.2(1)	ϵ_{297nm} 6550, ϵ_{588nm} 288				
$[Cu(N\text{-}Me_7sar)]^{3+}$	2.5(1), 9.0(1)	ϵ_{301nm} 6200, ϵ_{590nm} 310				

[a] Extinction coefficients in M^{-1} cm^{-1} and spectrum measured in water unless otherwise specified. [b] Value at 298 K. [c] Upper bound only. Leaders indicate that the value was unable to be determined from the available data.

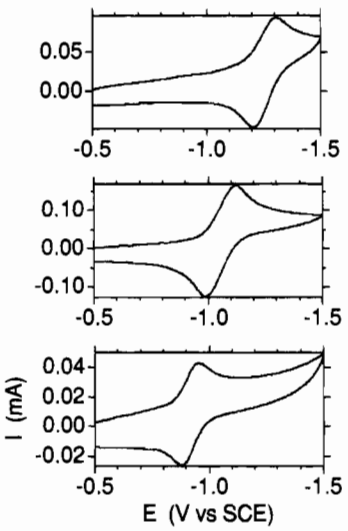

Figure 5. Cyclic Voltammograms of $[Ni(N\text{-}Me_5sar)]^{2+}$ (top), $[Ni(N\text{-}Me_6sar)]^{2+}$ (center) and $[Ni(N\text{-}Me_7sar)]^{3+}$ (bottom) (scan rate 1 V s^{-1}).

Table 9. Electrochemical Data

	scan rate[b]	pH 7			pH 1[a]		
		$E_{1/2}$[c]	ΔE_p[d]	i_a/i_c	$E_{1/2}$	ΔE_p	i_a/i_c
$[Ni(N\text{-}Me_5sar)]^{2+}$	100	−1.26	100	1.0		...	...
	1000		150	1.0	−1.13	...	...
	10000		290	1.0		140	1.0
$[Ni(N\text{-}Me_6sar)]^{2+}$	100	−1.05	90	1.0		90	...
	1000		150	1.0	−0.92	100	...
	10000		290	1.0		150	0.81
$[Ni(N\text{-}Me_7sar)]^{3+}$	100	−0.91	80	1.0		...	...
	1000		100	1.0	−0.91	...	...
	10000		180	1.0		180	1.0
$[Cu(N\text{-}Me_5sar)]^{2+}$	100	−0.78	80	0.84	...	...	0.0
	1000		110	0.91	...	...	0.0
	10000		210	1.0	...	...	0.0
$[Cu(N\text{-}Me_6sar)]^{2+}$	100	−0.65	70	0.93	...	...	0.0
	1000		90	1.0	...	...	0.0
	10000		170	1.0	...	...	0.0
$[Cu(N\text{-}Me_7sar)]^{3+}$	100	−0.53	70	0.45	...	...	0.0
	1000		100	0.91	...	...	0.0
	10000		190	1.0	...	...	0.0

[a] Leaders indicate the value was undetermined due to the proximity of the couple to the H^+ reduction wave (Ni(II) Complexes) or rapid dissociation of the reduced species (Cu(II) complexes). [b] mV s^{-1}. [c] V vs SCE. [d] mV.

Aqueous cyclic voltammetry of the three Ni(II) complexes at pH 7 (Figure 5) defined quasi-reversible Ni(II/I) redox couples, with each putative Ni(I) complex being quantitatively reoxidized during the timescale of the experiment. The data are summarized in Table 9. The presence of four coordinated tertiary amines in $[Ni(N\text{-}Me_6sar)]^{2+}$, as opposed to three in $[Ni(N\text{-}Me_5sar)]^{2+}$, results in a relative stabilization of the monovalent complex by 210 mV. Cyclic voltammetry conducted at pH 1 gave a similar result, although the $E_{1/2}$ values for $[Ni(HN\text{-}Me_5sar)]^{3+}$ and $[Ni(HN\text{-}Me_6sar)]^{3+}$ were shifted by *ca.* +120 mV due to protonation of one free amine. There was no shift in the $E_{1/2}$ value for $[Ni(N\text{-}Me_7sar)]^{3+}$, indicating that protonation of the single free amine still had not occurred at pH 1.

Copper(II) Complexes. By contrast with the Ni(II) system, chromatographic separation of $[Cu(N\text{-}Me_5sar)]^{2+}$ and $[Cu(N\text{-}Me^6sar)]^{2+}$ was only achieved with $NaClO_4$ solution as eluent, although only relatively small amounts of the mixture could be separated at a time due to the very similar chromatographic behavior of its components. If both species were present in concentrated perchlorate solution, then co-crystallization occurred. It was found that an equilibrium between the perchlorato and aqua complexes of both $[Cu(N\text{-}Me_5sar)]^{2+}$ and $[Cu(N\text{-}Me_6sar)]^{2+}$ was established during ion exchange chromatography when $NaClO_4$ solution was employed as eluent. The leading bands of $[Cu(N\text{-}Me_5sar)(OClO_3)]^+$ and $[Cu(N\text{-}Me_6sar)(OClO_3)]^+$ became more intense relative to the trailing fractions (of $[Cu(N\text{-}Me_5sar)(OH_2)]^{2+}$ and $[Cu(N\text{-}Me_6sar)(OH_2)]^{2+}$) when the concentration of the eluent was increased.

The X-ray crystallographic analysis of $[Cu(N\text{-}Me_5sar)](ClO_4)_2$ (Figure 6) revealed a distorted square-pyramidal geometry of the complex cation, with the ligand coordinating as a tetradentate in addition to one weakly bound perchlorate in the apical site. As was found in the structure of $[Ni(N\text{-}Me_5sar)](ClO_4)_2$, the lone secondary amine in $[Cu(N\text{-}Me_5sar)(OClO_3)]^+$ is coordinated and exhibits a significantly shorter Cu-N bond length than do the remaining Cu-$N(CH_3)$ bonds, but both are typical of secondary or tertiary amine copper(II) complexes.[28,29] There was no significant tetrahedral distortion of the plane of four N-donors. The conformation of the ligand is the same as found in the structure of $[Ni(N\text{-}Me_5sar)](ClO_4)_2$.

The structure of $[Cu(N\text{-}Me_7sar)](ClO_4)_3{\cdot}0.5H_2O$ was also determined by X-ray analysis and a drawing of the cation is shown in Figure 7. As was found in the structure of $[Cu(N\text{-}Me_5sar)](ClO_4)_2$, one perchlorate anion is coordinated in the apical site, although the Cu-O(11) bond length in $[Cu(N\text{-}Me_7sar)(OClO_3)]^{2+}$ is *ca.* 0.25 Å shorter. The CuN_4 plane in $[Cu(N\text{-}Me_7sar)(OClO_3)]^{2+}$ is significantly more distorted than in the structure of $[Cu(N\text{-}Me_5sar)(OClO_3)]^+$ with the Cu-atom being displaced by 0.25 Å from the basal N_4 plane toward O(11), in addition to a significant tetrahedral distortion of 0.04(1) Å. The conformation of the ligand is similar to that exhibited by the $[Ni(N\text{-}Me_5sar)]^{2+}$ and $[Ni(HN\text{-}Me_6sar)]^{3+}$ cations, where the five-membered chelate rings have opposite chiralities and the

(28) Azuma, N.; Kohno, Y.; Nemoto, F.; Kajikawa, Y.; Ishizu, K.; Takakuwa, T.; Tsuoyama, S.; Tsuboyama, K.; Kobayashi, K.; Sakurai, T. *Inorg. Chim. Acta* **1994**, *215*, 109.
(29) Comba, P.; Curtis, N. F.; Lawrance, G. A.; O'Leary, M. A.; Skelton, B. W.; White, A. H. *J. Chem. Soc., Dalton Trans.* **1988**, 2145.

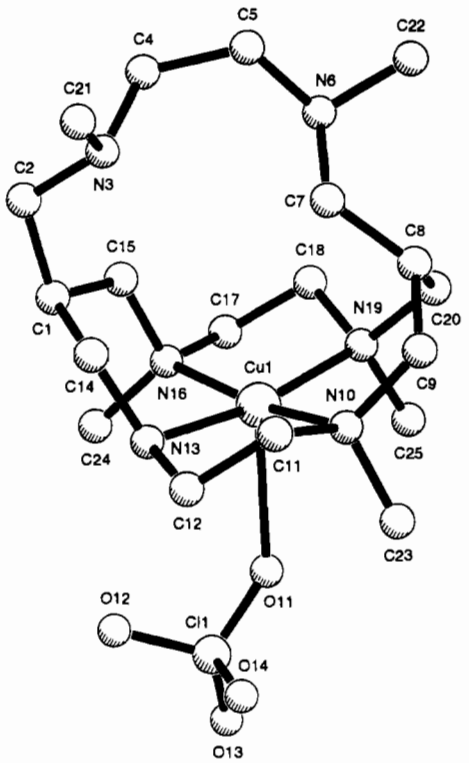

Figure 6. Drawing of $[Cu(N\text{-}Me_5sar)(OClO_3)]^+$.

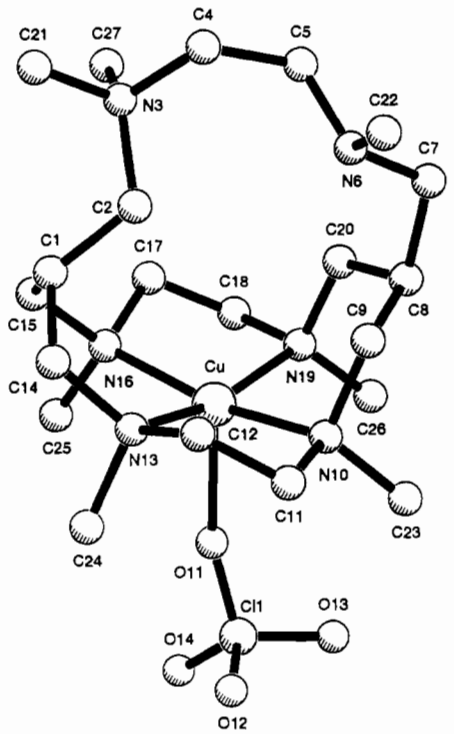

Figure 7. Drawing of $[Cu(N\text{-}Me_7sar)(OClO_3)]^{2+}$.

six-membered chelate rings adopt one chair and one boat conformer. It is apparent that the conformations of the five- and six-membered chelate rings are dependent on each other.

The aqueous solution electronic spectra of the three Cu(II) complexes (Table 8) are consistent with a square-pyramidal geometry with solvation occurring in the apical site.[30] The effect of N-methylation of the coordinated amines on the electronic spectrum is to weaken the ligand field as seen in the hypsochromic shift of the single visible maximum on going from $[Cu(N\text{-}Me_5sar)]^{2+}$ to $[Cu(N\text{-}Me_6sar)]^{2+}$. Deprotonation of the aqua ligand of $[Cu(N\text{-}Me_7sar)(OH_2)]^{3+}$ (pK_a 9.0) did not have a significant effect on the electronic spectrum. The invariance of the spectrum despite deprotonation of a coordinated ligand is not surprising since the oxygen is only weakly bound in the first instance, as a result of the pseudo Jahn–Teller effect.[30] Therefore, deprotonation results in a relatively minor perturbation of the overall ligand field strength. Similarly, the anticipated differences in the $Cu-OH_2$ bond lengths of the solvated $[Cu(N\text{-}Me_5sar)(OClO_3)]^+$ and $[Cu(N\text{-}Me_7sar)(OClO_3)]^{2+}$ ions are of little consequence with respect to the electronic spectra by comparison with changes in the CuN_4 environment. The same aqua/hydroxy pK_a values for $[Cu(N\text{-}Me_5sar)(OH_2)]^{2+}$ and $[Cu(N\text{-}Me_6sar)(OH_2)]^{2+}$ were too high to be measured potentiometrically. By analogy with the Ni(II) systems, the pK_a values for the three Cu(II) complexes in the range $2 < pK_a < 7$ were assigned to free tertiary amine deprotonations.

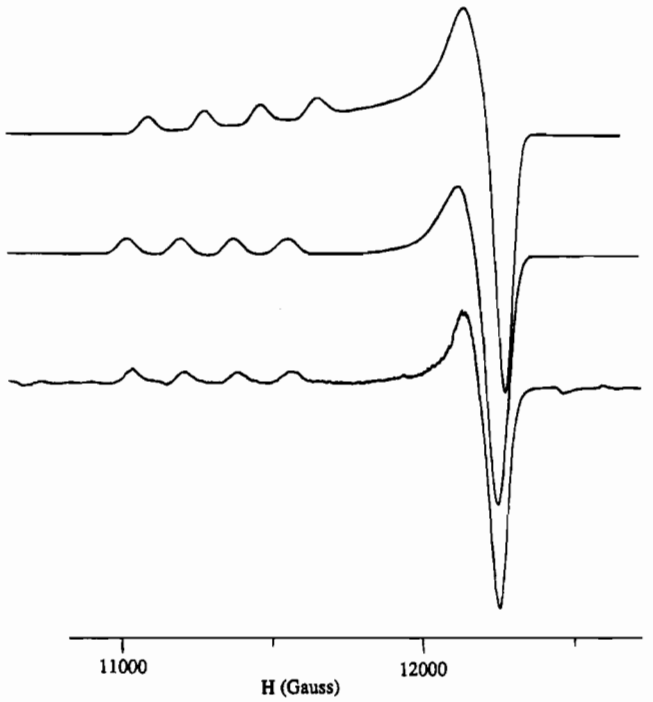

Figure 8. Q-Band EPR Spectra of (a) $[Cu(N\text{-}Me_5sar)]^{2+}$ (top), $[Cu(N\text{-}Me_6sar)]^{2+}$ and $[Cu(N\text{-}Me_7sar)]^{3+}$ (bottom) at 40 K.

The frozen solution EPR spectra of the three Cu(II) complexes (Figure 8) are typical of d^9 complexes with pseudo-axial symmetry.[31] The spin Hamiltonian parameters were obtained by computer simulation of the experimental spectra and are as follows: $[Cu(N\text{-}Me_5sar)]^{2+}$ $g_{\|}$ 2.195(2), $g_\perp$ 2.044(2), $A_{\|}$ 187(1) G, $A_\perp$ 25(5) G; $[Cu(N\text{-}Me_6sar)]^{2+}$ $g_{\|}$ 2.214(2), $g_\perp$ 2.048(2), $A_{\|}$ 178(1) G, $A_\perp$ 25(5) G; $[Cu(N\text{-}Me_7sar)]^{3+}$ $g_{\|}$ 2.211(2), $g_\perp$ 2.047-(2), $A_{\|}$ 175(1) G, $A_\perp$ 25(5) G. The EPR spectrum of $[Cu(N\text{-}Me_7sar)]^{3+}$ was very similar to that of $[Cu(N\text{-}Me_6sar)]^{2+}$. Coupled with the similarity of their solution electronic spectra, this indicates that the geometries of the two chromophores in solution are essentially the same. The larger $A_{\|}$ and smaller $g_{\|}$ value of $[Cu(N\text{-}Me_5sar)]^{2+}$ is indicative of a more planar CuN_4 chromophore[32] in solution than that found in $[Cu(N\text{-}Me_6sar)]^{2+}$ or $[Cu(N\text{-}Me_7sar)]^{3+}$, and this is consistent with the observations from the crystal structures.

The aqueous cyclic voltammograms of all Cu(II) complexes at pH 7 (Figure 9) each exhibit single, quasi-reversible Cu(II/I)

(30) Hathaway, B. J. *Struct. Bonding* **1984**, *57*, 55.

(31) Hathaway, B. J. *Coord. Chem. Rev.* **1970**, *5*, 1.

(32) Miyoshi, K.; Tanaka, H.; Kimura, E.; Tsuboyama, S.; Murata, S.; Shimizu, H.; Ishizu, K. *Inorg. Chim. Acta* **1983**, *78*, 23.

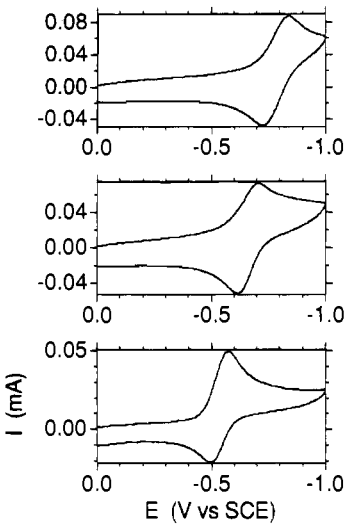

Figure 9. Cyclic Voltammograms of $[Cu(N\text{-}Me_5sar)]^{2+}$ (top) $Cu(N\text{-}Me_6sar)]^{2+}$ (center) $[Cu(N\text{-}Me_7sar)]^{3+}$ (bottom) (scan rate 1 V s^{-1}).

Scheme 1. Mechanism for Reduction of Cu(II) Complexes

$$[Cu^{II}L]^{m+} \overset{e^-}{\rightleftharpoons} [Cu^{I}L]^{(m-1)+}$$

$$[Cu^{I}L]^{(m-1)+} \overset{k_d}{\rightleftharpoons} Cu^{I}_{aq} + L$$

$$1/2[\,2\,Cu^{I}_{aq} \xrightarrow{k_{disp}} Cu^{II}_{aq} + Cu\,]$$

$$1/2[\,Cu^{II}_{aq} \xrightarrow{2\,e^-} Cu\,]$$

L = N-Me_5sar, N-Me_6sar (m=2), N-Me_7sar^+ (m=3).

waves. In each case, the cyclic voltammograms became more reversible, i.e. i_{pa}/i_{pc} approached unity, with increasing scan rate; which was indicative of a chemical reaction following electron transfer (EC mechanism). Partial dissociation, or at least rearrangement, of each Cu(I) complex occurs during the voltammetric experiment. The first-order rate constants at pH 7 for these processes, determined from the scan rate dependence of the current ratios,[33] are: $[Cu(N\text{-}Me_5sar)]^+$, k_d 6(1) × 10^{-2} s^{-1}, $Cu(N\text{-}Me_6sar)]^+$, k_d 2(1) × 10^{-2} s^{-1} and $[Cu(N\text{-}Me_7sar)]^{3+}$, k_d 2.6(4) × 10^{-1} s^{-1}. The electrochemical data are summarized in Table 9. Cyclic voltammetry of all complexes at pH 1 (ClO_4^- medium) resulted in totally irreversible cathodic waves (scan rate 1 V s^{-1}). The acidic conditions evidently accelerate dissociation of the labile Cu(I) complexes (k_d > 100 s^{-1}).

Bulk electrolysis of all Cu(II) complexes at −1.0 V vs SCE over a mercury pool resulted in the passage of two electrons per mole of complex. Since the voltammetric experiments established that each Cu(I) complex was not stable in aqueous solution, this is consistent with a single-electron reduction to the Cu(I) complex which dissociates relatively quickly ($3 \leq t_{1/2} \leq 30$ s), then the liberated Cu_{aq}^+, or the half equivalent of Cu_{aq}^{2+} formed as a result of rapid disproportionation, is reduced in another single-electron process (Scheme 1). Significantly, there was a residual blue or purple colour (indicative of Cu(II) species) in all solutions after the passage of one electron per mole of complex, which is consistent with dissociation of the monovalent complexes (seconds) occurring at a faster rate than that of the bulk electrolysis experiment (hours).

Discussion

In order that inversion of the coordinated tertiary amine may occur, the M−N bond must be broken, so there must be either a competing ligand,[7,34] or a Lewis acid, that will maintain the break, at least temporarily. Interconversion of N-based diastereomers may then only occur if the lifetime of the dissociated N-atom is long relative to the half-life for its inversion. As a result, N-based isomerization of a coordinated tertiary amine is typically slow, and the outcome of ligand substitution reactions involving polydentate tertiary amines is often dominated by kinetics rather than the relative stabilities of the possible isomers. By contrast, inversion of secondary amine relatives is facile and may occur while the amine is not coordinated in labile complexes or through inversion of the deprotonated N-donor for highly-charged, inert complexes. Here it appeared that all complexes reported existed in but one N-based isomeric form, i.e. *trans-I*, and no isomeric interconversion was identified. It appears that the presence of the noncoordinated straps in N-Me_5sar, N-Me_6sar and N-Me_7sar^+ dictates this configuration. That is, the two six-membered chelate rings are constrained to be on the same side of the MN_4 plane, and as a result, the four methyl groups bound to the coordinated N-atoms are required to lie on the opposite side of the plane.

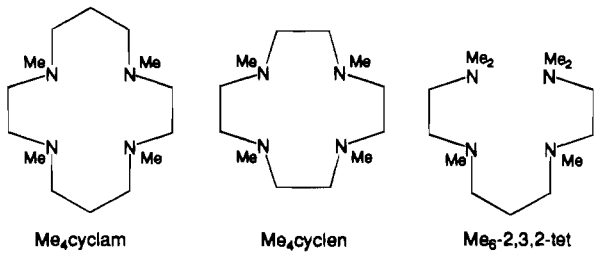

It has been well established that N-methylation of coordinated amines results in a positive shift in the M(II/I) redox couple of the complex, i.e. the lower oxidation state is stabilized relative to its unmethylated parent,[35−37] and this is consistent with the relative $E_{1/2}$ values of Cu(II) and Ni(II) systems here. There have been several proposals put forward in an effort to explain the observed shifts in the redox couple upon N-methylation. It has been suggested that the monovalent complex is stabilized by N-methylation relative to secondary amine analogues as a result of (i) an increase in the preferred cavity size of the macrocycle which is more compatible with the larger M^+ ion;[38] (ii) increased hydrophobicity which stabilizes the lower charge of the reduced complex;[39] and (iii) out-of-plane distortions resulting from non-bonded repulsion of the N-methyl groups which favor coordination geometries, e.g. tetrahedral, more characteristic of the low-valent complex.[40] When the results in Table 8 and the crystal structures reported herein are examined, it appears that point (i) is most consistent with our observations. The M−N(H) bond length in $[M(N\text{-}Me_5sar)]^{2+}$ (M = Cu or Ni) is significantly shorter than the three remaining M−N(CH_3) bond lengths and those in $[M(N\text{-}Me_7sar)]^{3+}$, so the steric effects of N-methylation clearly increase the M(II)-N bond length despite the stronger basicity of the tertiary amine.

(33) Nicholson, R. S.; Shain, I. *Anal. Chem.* **1964**, *36*, 706.
(34) Moore, P.; Sachinidis, J.; Willey, G. R. *J. Chem. Soc., Chem. Commun.* **1983**, 522.
(35) Jubran, N.; Ginzburg, G.; Cohen, H.; Koresh, Y.; Meyerstein, D. *Inorg. Chem.* **1985**, *24*, 251.
(36) Blake, A. J.; Gould, R. O.; Hyde, T. I.; Schröder, M. *J. Chem. Soc., Chem. Commun.* **1987**, 431.
(37) Ciampolini, M.; Fabbrizzi, L.; Licchelli, M.; Perotti, A.; Pezzini, F.; Poggi, A. *Inorg. Chem.* **1986**, *25*, 4131.
(38) Barefield, E. K.; Freeman, G. M.; van Derveeer, D. G. *Inorg. Chem.* **1986**, *25*, 552.
(39) Golub, G.; Cohen, H.; Meyerstein, D. *J. Chem. Soc., Chem. Commun.* **1992**, 397.
(40) Blake, A. J.; Gould, R. O.; Hyde, T. I.; Schröder, M. *J. Chem. Soc., Chem. Commun.* **1987**, 1730.

Although genuine structural reports of tetra-aza macrocyclic complexes of nickel(I)[41] are few, an extension of the Ni−N bond length upon reduction is anticipated. Therefore an expansion of the preferred cavity size of the macrocycle will tend to stabilize the larger monovalent ion. Similar arguments apply for the Cu(II/I) systems, although there are no known crystal structures of tetra-aza macrocyclic copper(I) complexes. The crystal structures of $[Ni(HN\text{-}Me_6sar)]^{3+}$ and $[Ni(N\text{-}Me_7sar)]^{3+}$ reveal a significant tetrahedral distortion of their NiN_4 moieties whereas the N-donors in $[Ni(N\text{-}Me_5sar)]^{2+}$ are coplanar. However, the d^9 Ni(I) complexes, by analogy with their isoelectronic Cu(II) relatives, should prefer to adopt planar or tetragonally elongated geometries, so the observed tetrahedral distortions of $[Ni(HN\text{-}Me_6sar)]^{3+}$ and $[Ni(N\text{-}Me_7sar)]^{3+}$ alone should not significantly stabilize their monovalent complexes relative to $[Ni(N\text{-}Me_5sar)]^{2+}$. The tetrahedral distortion defined in the crystal structure $[Cu(N\text{-}Me_7sar)(OClO_3)]^{2+}$ was rather small and, like the Ni(II) systems, this cannot be solely responsible for the shift of the Cu(II/I) redox couple relative to the $[Cu(N\text{-}Me_5sar)]^{2+}$ and $[Cu(N\text{-}Me_6sar)]^{2+}$. In both of the Ni(II) and Cu(II) systems, the higher charge of the $[M(N\text{-}Me_7sar)]^{3+}$ ions results in a comparable positive shift in the M(II/I) redox couple to that effected by substitution of a coordinated secondary amine H-atom by a methyl group.

The electrochemical results of the copper complexes deserve some comment in relation to other related N-methylated analogues. In the case of $[Cu(Me_4cyclen)]^{2+}$, and its tetrabenzylated analogue, cyclic voltammetry resulted in two waves of unequal intensity.[42] Bulk electrolysis, in acetonitrile, showed that these two waves sum to a single electron process, although no explanation could be offered for this observation. Concerning the voltammetry of $[Cu(Me_6\text{-}2,3,2\text{-}tet)]^{2+}$,[39] the two close running waves were each assigned as being single-electron processes, although no bulk electrolysis data were supplied to support this assertion. In neither of these reports was chromatographic separation of the Cu(II) complexes attempted. A rather similar voltammogram is obtained from the co-crystallized mixture of $[Cu(N\text{-}Me_5sar)]^{2+}$ and $[Cu(N\text{-}Me_6sar)]^{2+}$. Possibly, in the cases of $[Cu(Me_4cyclen)]^{2+}$ and $[Cu(Me_6\text{-}2,3,2\text{-}tet)]^{2+}$, there are complexes of other N-methylated ligands, e.g. Me_3-cyclam or Me_5-2,3,2-tet, present in solution, which naturally exhibit slightly different $E_{1/2}$ values from the Cu(II) complexes of their tetra-tertiary amine relatives. The difficulty experienced in separating $[Cu(N\text{-}Me_5sar)]^{2+}$ from $[Cu(N\text{-}Me_6sar)]^{2+}$ would probably be also met with the Cu(II) complexes of the N-methylated cyclam and 2,3,2-tet systems if the ligands had not been rigorously purified.

The thermodynamic data obtained from the temperature dependence of the $[Ni(N\text{-}Me_6sar)]^{2+}$ and $[Ni(N\text{-}Me_7sar)]^{3+}$ electronic spectra in water (Table 8) are the same within experimental error. The negative $\Delta S°$ and $\Delta H°$ values show that exothermic adduct formation is occurring, which is a general trend in the solvation of tetraamine nickel(II) complexes.[24-27] Indeed the values are similar to those reported for the aqueous solvation of the macromonocyclic analogue *R,S,R,S*-$[Ni(Me_4cyclam)]^{2+}$,[24] where coordination of a single solvent molecule was also observed. The incoming solvent molecule undoubtedly coordinates in a manner similar to that of the perchlorate anion in $[Cu(N\text{-}Me_5sar)(OClO_3)]^{+}$ and $[Cu(N\text{-}Me_7sar)(OClO_3)]^{2+}$ or the monodentate ligand in the structurally characterized high-spin, five-coordinate adducts *R,S,R,S*-$[Ni(Me_4cyclam)(X)]^{n+}$ (X = N_3^-,[43] DMF[27]). The observed displacement of the Ni-atom from the basal N_4 plane in the square-planar cations $[Ni(N\text{-}Me_5sar)]^{2+}$, $[Ni(HN\text{-}Me_6sar)]^{3+}$ and $[Ni(N\text{-}Me_7sar)]^{3+}$ is a consequence of the *trans-I* configuration, although axial coordination does augment this out of plane distortion as shown in the structures of $[Cu(N\text{-}Me_5sar)(OClO_3)]^{+}$ and $[Cu(N\text{-}Me_7sar)(OClO_3)]^{2+}$. As a result, the binding of a second solvent molecule in the site *trans* to the first is blocked by steric interactions with the ligand. The rather small cavity formed by the bridging, noncoordinated strap in tetradentate coordinated complexes of N-Me_6sar and N-Me_7sar^+ also inhibits *trans* approach by a second solvent molecule. These complexes bear an obvious structural similarity to the so-called lacunar macrocycles.[44]

Scheme 2. Spin and Protonation Equilibria for Ni(II) Complexes

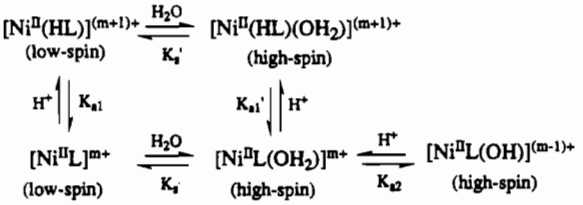

L = N-Me_5sar, N-Me_6sar (m=2), N-Me_7sar^+ (m=3).

By contrast, the variation of the electronic spectra of $[Ni(N\text{-}Me_5sar)]^{2+}$ in the three solvent systems as a function of temperature was modest. In fact, there was little evidence to suggest that there was any significant increase in the amount of high-spin $[Ni(N\text{-}Me_5sar)]^{2+}$ upon warming. Although there was a slight decrease in absorbance of the single visible band when the temperature was raised, there was no significant complementary increase in absorbance in the 550 and 380 nm regions which would indicate the formation of a high-spin complex. In this case, the decrease in absorbance is attributable to line broadening through thermal vibrational excitation. The reluctance of $[Ni(N\text{-}Me_5sar)]^{2+}$ to coordinate a solvent molecule is unexpected, particularly considering the fact that the Ni-atom is already displaced from the basal N_4 plane to accept a potential axially coordinating ligand, as defined by the X-ray crystallographic analysis. The main structural difference between $[Ni(N\text{-}Me_5sar)]^{2+}$ and the tetra-tertiary amine $[Ni(N\text{-}Me_6sar)]^{2+}$ and $[Ni(N\text{-}Me_7sar)]^{3+}$ ions is in the tetrahedral distortion of the NiN_4 chromophores. It appears that, in this case, the tetrahedral distortion, but not the displacement of the Ni-atom from the N_4 plane distortion, enhances the formation of the five-coordinate solvated adduct.

Nevertheless, in aqueous solution the high-spin form was identified indirectly during the potentiometric titration through deprotonation of the aqua ligand (pK_a 10.6). The relevant spin and protonation equilibria for the Ni(II) complexes in aqueous solution are described in Scheme 2. It can be seen that although the spin equilibrium (K_s) strongly favors the low-spin form of $[Ni(N\text{-}Me_5sar)]^{2+}$, upon raising the pH this equilibrium is disturbed by deprotonation of the aqua ligand of the high-spin form (K_{a2}). The scheme also illustrates that, in principle, there are two distinct pK_a values for the deprotonation of the free amine in the high- and low-spin forms, i.e. K_{a1} and K_{a1}', and two spin-equilibrium constants. However, the equilibria in Scheme 2 are established too rapidly to allow separate deter-

(41) Furenlid, L. R.; Renner, M. W.; Szalda, D. J.; Fujita, E. *J. Am. Chem. Soc.* **1991**, *113*, 883.
(42) Webb, R. L.; Mino, M. L.; Blinn, E. L.; Pinkerton, A. A. *Inorg. Chem.* **1993**, *32*, 1396.
(43) D'Aniello, M. J., Jr.; Mocella, M. T.; Wagner, F.; Barefield, E. K.; Paul, I. C. *J. Am. Chem. Soc.* **1975**, *97*, 192.
(44) Herron, N.; Cameron, J. H.; Neer, G. L.; Busch, D. H. *J. Am. Chem. Soc.* **1983**, *103*, 298.

mination of K_{a1} and K_{a1}', and moreover one cannot say to which protonation reaction the observed K_a belongs. The fact that the electronic spectra of all Ni(II) complexes are essentially unchanged regardless of whether the free amines are protonated or not indicates that K_{a1} and K_{a1}' are quite similar, as are K_x and K_x'. Although the three Ni(II) complexes in this work exhibited quite different spin equilibria, all were crystallized in the low-spin form. This is notable since all structures of [Ni(Me$_4$cyclam)]$^{2+}$ have been of high-spin adducts with either square-pyramidal or tetragonally distorted octahedral geometries being defined.[27,43,45]

It has been established that hexadentate coordination of N-Me$_6$sar, or N-Me$_5$sar, to Ni(II) or Cu(II) was not achieved. However, this could be a consequence of slow kinetics 'trapping' the complexes in configurations that inhibited hexadentate coordination, or simply that the hexaamine complexes were genuinely too unstable relative to the tetradentate coordinated complexes. With the aid of molecular mechanics, one can make predictions as to the structure of the putative hexadentate coordinated [Ni(N-Me$_6$sar)]$^{2+}$ complex, and to the likelihood of forming hexadentate coordinated complexes with other metal ions. The strain energy minimized structure of hexadentate coordinated [Ni(N-Me$_6$sar)]$^{2+}$ is shown in Figure 10. The predicted Ni–N bond length of the D_3-symmetric cation is 2.25 Å, which is longer than any known Ni(II)-N(amine) bond length, and the trigonal twist angle ϕ is 38° (where $\phi = 60°$ for octahedral and $\phi = 0°$ for trigonal prismatic geometry). These values contrast with those determined in the X-ray crystal structure of a secondary amine analogue, [Ni((NH$_3$)$_2$sar)](NO$_3$)$_4$,[46] where Ni–N$_{av}$ is 2.11(1) Å and ϕ is 47°. Given that the predicted distortions of the Ni–N bond lengths and the trigonal twist angle in hexacoordinated [Ni(N-Me$_6$sar)]$^{2+}$ are so large, qualitatively, it would be surprising if such a complex could be isolated, although the present calculations make no predictions as to the dissociation energy of the molecule. A particularly helpful molecular mechanics calculation for complexes of polydentate ligands is the determination of preferred hole, or cavity, sizes. A plot of the ligand strain energy as a function of the M–N bond length for hexadentate coordinated [M(N-Me$_6$sar)]$^{n+}$ and tetradentate coordinated [M(N-Me$_6$sar)(OH$_2$)]$^{n+}$ is also shown in Figure 10. It is clear that the ideal M–N bond length for minimization of intraligand strain in the hexadentate coordinated complex is *ca.* 2.38 Å, and the majority of transition metal ions will prefer much shorter M–N bond lengths. Moreover, the flexibility of the ligand when coordinated as a tetradentate is clearly greater as can be seen in the relative steepness of the two curves. It emerges from these calculations that this tetradentate mode of coordination is more tolerant of metal ions which do not match the preferred hole size of the ligand, i.e. Ni(II) and Cu(II), than that of hexadentate

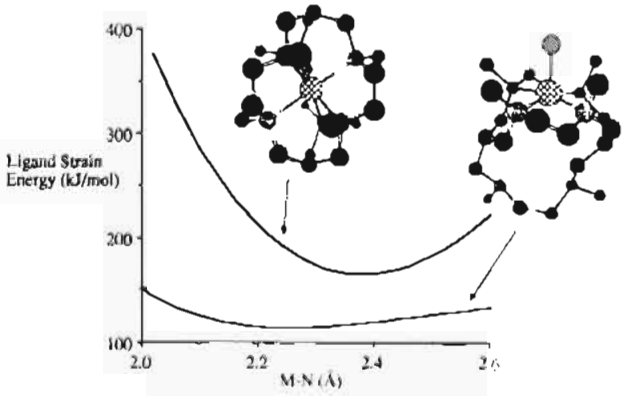

Figure 10. Ligand Strain Energy (kJ mol^{-1}) as a Function of the M–N Bond Length (Å) for Hexadentate and Tetradentate Coordinated [M(N-Me$_6$sar)]$^{n+}$.

coordinated analogues, although we cannot make any assertions as to the relative stabilities of the two modes of coordination at present. Coupled with the apparent tendency of [M(N-Me$_6$sar)]$^{n+}$ toward large trigonal twist distortions, which would be opposed by transition metal ions with strong preferences for octahedral geometry, it is evident that hexadentate coordinated complexes of large metal ions with little or no electronic preference for octahedral symmetry, e.g. Cd(II) or Hg(II), will be best suited to bind N-Me$_6$sar as a hexadentate and this goal is currently being pursued.

Conclusions

The present study has shown that hexadentate coordination of the macrobicyclic hexaamines N-Me$_6$sar or N-Me$_5$sar to either Cu(II) or Ni(II) is disfavored relative to tetradentate coordination. Molecular mechanics calculations indicate that the reluctance for either Cu(II) or Ni(II) to coordinate N-Me$_6$sar as a hexadentate is a result of a mismatch between the preferred M–N bond lengths of the ligand (*ca.* 2.38 Å) and those of the metal ions (*ca.* 1.90–2.10 Å). Therefore, despite the encapsulating potential of the secondary amine parent sar, the Cu(II) and Ni(II) complexes of N-Me$_6$sar behave in an analogous manner to macromonocyclic relatives. The trends shown by the complexes of N-Me$_5$sar, N-Me$_6$sar and N-Me$_7$sar$^+$ are consistent with N-methylation of coordinated amines resulting in (i) a positive shift in the $M^{III/II}$ redox couple; (ii) lengthening of the M–N bond which results in a weakening of the ligand field, as expected.

Acknowledgment. We thank Dr. R. Bramley for assistance with the EPR measurements, and D. Bogsanyi for performing the potentiometric titrations. Financial support of the Australian Research Council is gratefully acknowledged.

Supplementary Material Available: Unit cell drawings, and tables of complete atomic coordinates, bond lengths and angles, thermal parameters, torsional angles, nonbonded contacts, least squares planes, and crystal data for all structures (128 pages). Ordering information is given on any current masthead page.

(45) Wagner, F.; Mocella, M. T.; D'Aniello, M. J., Jr.; Wang, A. H.-J.; Barefield, E. K. *J. Am. Chem. Soc.* **1974**, *96*, 2625.
(46) Clark, I. J.; Creaser, I. I.; Engelhardt, L. M.; Harrowfield, J. M.; Krausz, E. R.; Moran, G. M.; Sargeson, A. M.; White, A. H. *Aust. J. Chem.* **1993**, *46*, 111.